



Research

Cite this article: Stankowski S, Streisfeld MA. 2015 Introggressive hybridization facilitates adaptive divergence in a recent radiation of monkeyflowers. *Proc. R. Soc. B* **282**: 20151666. <http://dx.doi.org/10.1098/rsob.2015.1666>

Received: 13 July 2015

Accepted: 3 August 2015

Subject Areas:
evolution

Keywords:
adaptation, speciation, hybridization, *Mimulus*, flower colour

Author for correspondence:
Matthew A. Streisfeld
e-mail: mstreis@uoregon.edu

Electronic supplementary material is available at <http://dx.doi.org/10.1098/rsob.2015.1666> or via <http://rsob.royalsocietypublishing.org>.

Introggressive hybridization facilitates adaptive divergence in a recent radiation of monkeyflowers

Sean Stankowski and Matthew A. Streisfeld

Institute of Ecology and Evolution, University of Oregon, Eugene, OR 97403, USA

A primary goal in evolutionary biology is to identify the historical events that have facilitated the origin and spread of adaptations. When these adaptations also lead to reproductive isolation, we can learn about the evolutionary mechanisms contributing to speciation. We reveal the complex history of the gene *MaMyb2* in shaping flower colour divergence within a recent radiation of monkeyflowers. In the *Mimulus aurantiacus* species complex, red-flowered *M. a. ssp. puniceus* and yellow-flowered *M. a. ssp. australis* are partially isolated because of differences in pollinator preferences. Phylogenetic analyses based on genome-wide variation across the complex suggest two origins of red flowers from a yellow-flowered ancestor: one in *M. a. ssp. puniceus* and one in *M. a. ssp. flemingii*. However, in both cases, red flowers are caused by *cis*-regulatory mutations in the gene *MaMyb2*. Although this could be due to distinct mutations in each lineage, we show that the red allele in *M. a. ssp. puniceus* did not evolve *de novo* or exist as standing variation in its yellow-flowered ancestor. Rather, our results suggest that a single red *MaMyb2* allele evolved during the radiation of *M. aurantiacus* that was subsequently transferred to the yellow-flowered ancestor of *M. a. ssp. puniceus* via introggressive hybridization. Because gene flow is still possible among taxa, we conclude that introggressive hybridization can be a potent driver of adaptation at the early stages of divergence that can contribute to the origins of biodiversity.

1. Introduction

A primary goal in evolutionary biology is to identify the historical events that have led to adaptive differences between populations. Although recent studies have characterized the genetic changes underlying adaptation in several systems [1–5], the conditions surrounding the origins of adaptive alleles are rarely known. The classic view is that natural selection operates either on new mutations or on standing variation that is already present within populations [6–8]. However, despite controversy surrounding the importance of natural hybridization in evolution [9–14], it is becoming more widely appreciated that introggressive hybridization can promote adaptation by transferring advantageous alleles across taxonomic boundaries [15–24]. This is especially true in recent evolutionary radiations, such as in *Heliconius* butterflies and Darwin's finches [25–27], where gene flow among taxa has provided a fertile supply of beneficial genetic material that has allowed for rapid and repeated divergence. Thus, comprehensive analyses that distinguish among alternative historical scenarios are necessary for understanding the evolutionary mechanisms that are responsible for the origins of biodiversity.

Moreover, it is well known that reproductive isolation can evolve as a by-product of ecological adaptation to different environments [28–31]. Therefore, the processes of adaptation and speciation are often intimately linked, suggesting that if we can understand the origins of adaptations that contribute to reproductive isolation, we can learn about the history of speciation. However, speciation is a gradual process that can occur across a broad range of scenarios and spatial settings [32,33], potentially leading to a complex history of genetic changes underlying adaptive divergence. In addition, reproductive barriers continue to accumulate long after speciation is complete [34,35]. As a consequence, the traits and genes affecting isolation in extant species pairs may differ from when speciation

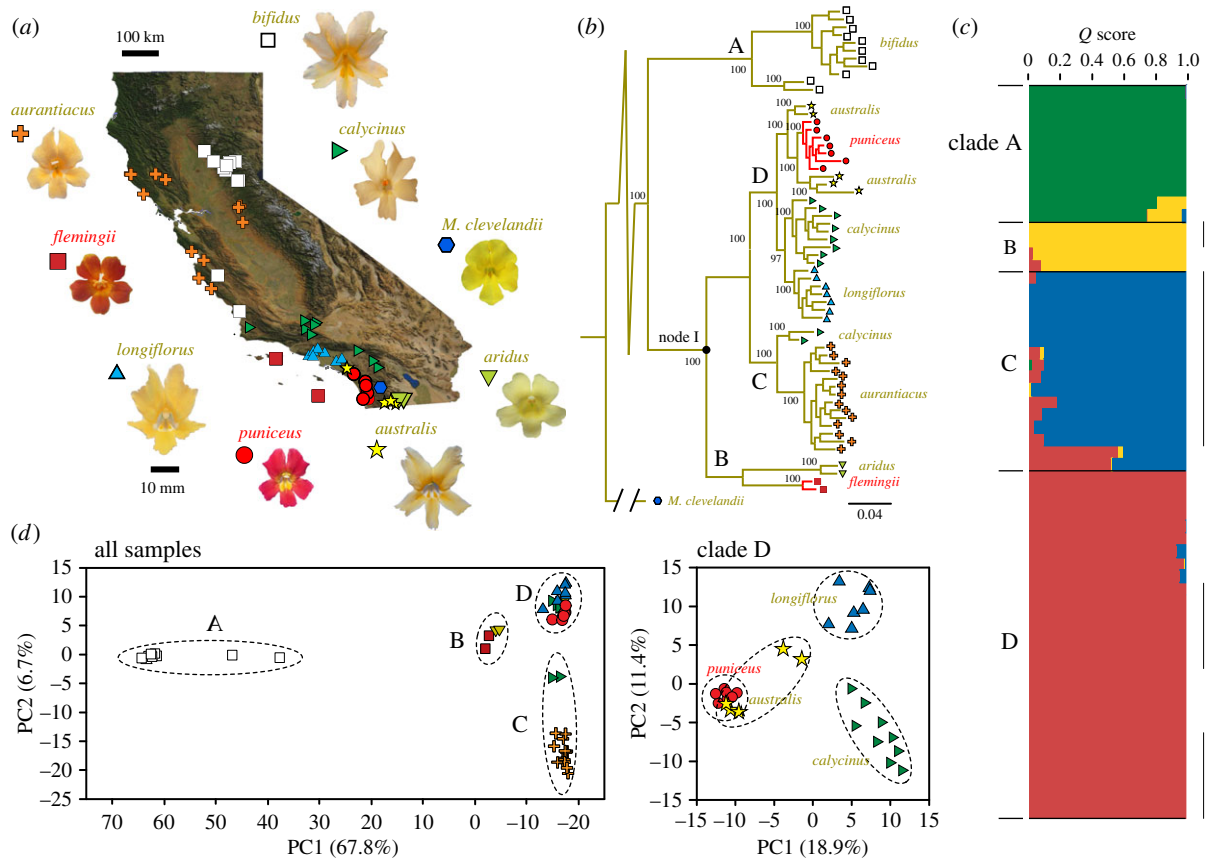


Figure 1. Evolutionary relationships within the *Mimulus aurantiacus* species complex. (a) Geographical locations of the 60 samples used for phylogenetic analysis, representing the eight subspecies of *M. aurantiacus* and the outgroup, *M. clevelandii*. Representative, standardized photographs of their flowers are presented. (b) Maximum-likelihood tree illustrating the relationships among the sampled individuals. Support values at all major nodes are indicated based on 100 bootstrap replicates. The four major clades (A–D) are indicated. Branches are coloured yellow to reflect the ancestral state (i.e. the probability of a character state transition at a node is less than 0.02). Branches are coloured red when the probability of a transition to red flowers (i.e. anthocyanins present) exceeded 0.98. (c) Bar plot showing the probability of membership (*Q* score) of each individual to one of four genotypic clusters, as revealed by the program *Structure* [37]. (d) Plots of the first two axes from principal components analyses (PCA) including either all ingroup samples (left) or only samples from Clade D (right). Dashed ellipses connect samples within clades (left) or within subspecies (right). The per cent variation explained by each axis is reported. (Online version in colour.)

commenced. By contrast, by studying taxa at an early stage of divergence, it is possible to investigate the evolutionary history of the genetic changes contributing to adaptation and reproductive isolation before they become confounded with other species differences.

The *Mimulus aurantiacus* species complex (Phrymaceae) is a recently radiated, monophyletic group of perennial shrubs comprising eight subspecies distributed mainly in California [36] (figure 1a). Despite being phenotypically and ecologically distinct from one another, all taxa in the complex are at least partially interfertile and hybridize in narrow areas if their geographical ranges overlap [38–42]. Of the traits that differ among the subspecies, variation in flower colour is the most striking, with two red-flowered subspecies and six yellow or yellow-orange-flowered subspecies occurring across the range of the complex (figure 1a).

In southern California, red-flowered *M. a. ssp. puniceus* and yellow-flowered *M. a. ssp. australis* co-occur in a narrow region where their geographical ranges overlap [42]. In a classic example of incipient speciation [43,44], pre-mating reproductive isolation has evolved between the subspecies largely as a by-product of ecological adaptation to different pollinators [42,45]. Specifically, hummingbird and hawkmoth pollinators rarely transition between flowers of each subspecies, resulting in strong, but incomplete pollinator isolation [42,45]. In support of the hypothesis that flower colour is adaptive and a

major driver of these preferences, geographical variation in flower colour is maintained despite ongoing gene flow at neutral loci [46]. Moreover, extensive genetic differentiation exists between the subspecies in *MaMyb2*, the gene primarily responsible for the transition in flower colour [47]. However, even though this group has had a long record of taxonomic study, the evolutionary relationships among subspecies and the number and direction of flower colour transitions are unresolved, making it difficult to infer the historical events that facilitated local adaptation.

In this study, we investigate the history of flower colour evolution in the *M. aurantiacus* complex. Using genome-wide variation, we produce the first resolved phylogeny for the complex and use ancestral state reconstructions to infer the order and number of flower colour transitions across the group. Although red flowers appear to have evolved twice from yellow-flowered ancestors, our genetic analyses revealed that red flowers in each lineage were caused by *cis*-regulatory mutations in the same gene, *MaMyb2*. While this could be due to independent mutations in each lineage, population genetic and genomic techniques show that the recent origin of red flowers in *M. a. ssp. puniceus* did not arise *de novo* or from ancestral variation retained in its yellow-flowered ancestor. Therefore, rather than arising twice as suggested by the phylogenetic analyses, our results indicate that a red *MaMyb2* allele arose once during the radiation of *M. aurantiacus* and was

shared with the ancestor of *M. a. ssp. puniceus* via introgressive hybridization. Thus, transitions from yellow to red flowers have a shared genetic basis that is shrouded by a complex history.

2. Results and discussion

(a) Analysis of genome-wide variation suggests two origins of red flowers

As an initial step towards understanding the history of flower colour evolution in the *M. aurantiacus* species complex, we used patterns of genome-wide variation to provide the first detailed, molecular account of the relationships among subspecies. We sequenced restriction-site associated DNA tags (RAD) across 60 populations from all eight subspecies and the out-group, *M. clevelandii*, and identified 41 528 SNPs that met our filtering requirements. Several methods of phylogenetic reconstruction (Bayesian, maximum-likelihood, neighbour joining and coalescent) were applied to these data, and all recovered well-supported topologies consisting of the same four clades (A–D in figure 1*b*; electronic supplementary material, figure S1). Additional non-tree-based approaches, including a Bayesian clustering algorithm (figure 1*c*) [37] and principal components analysis (PCA; figure 1*d*), recovered clusters of individuals that coincided with the major clades in the common tree topology. The four clades are moderately to highly differentiated from one another (range of between-clade F_{ST} : 0.30 to 0.75; range of proportion of fixed differences between clades: 0.004–0.305; electronic supplementary material, table S2), and similar to levels of differentiation reported for other recent evolutionary radiations [27,48,49].

Previously described taxa [41,50] generally formed reciprocally monophyletic groups within one of the four clades. Clade A consisted entirely of individuals of *M. a. ssp. bifidus* from northeastern and central California. Clade B included individuals from two subspecies, *M. a. ssp. aridus* from southeastern California and *M. a. ssp. flemingii* that is endemic to the Channel Islands off the California coast. Clade C comprised samples from *M. a. ssp. aurantiacus* and *M. a. ssp. calycinus* in central to northern California. *M. a. ssp. calycinus* was also found in the diverse Clade D from southern California, which also included *M. a. ssp. longiflorus*, *M. a. ssp. australis*, and *M. a. ssp. puniceus*. Pigment extractions revealed that only the red-flowered *M. a. ssp. puniceus* and *M. a. ssp. flemingii* produce red anthocyanin pigments in their corolla tissue, whereas the remaining subspecies do not, resulting in their yellow or yellow-orange flowers (electronic supplementary material, figure S2). Hereafter, we refer to taxa using only their subspecific names.

We draw two initial conclusions from these analyses that are pertinent for investigating the origins of flower colour differences. First, ancestral state reconstructions suggest that yellow flowers (i.e. anthocyanin absent) are ancestral in *M. aurantiacus*, with red flowers derived once in Clade B in the lineage leading to *flemingii* and once in Clade D in the lineage leading to *puniceus* (figure 1*b*). Thus, based on phylogenetic analyses, anthocyanins appear to have been gained independently in the flowers of each red-flowered subspecies. Our second conclusion is that *puniceus* and *australis* are each other's closest relatives. Samples of the red-flowered *puniceus* are nested within the clade of yellow-flowered *australis*, supporting the previous conclusion that *puniceus* and *australis* are at a very early stage in the speciation process [42].

(b) Red flowers in each subspecies are caused by *cis*-regulatory mutations in *MaMyb2*

Although *puniceus* and *flemingii* are distantly related within the *M. aurantiacus* complex, our genetic analyses indicate that their red flowers are caused by *cis*-regulatory mutations in the same gene. Previous work has shown that red flowers in *puniceus* are caused primarily by a *cis*-regulatory mutation in the R2R3-MYB transcription factor *MaMyb2*, which activates the expression of at least three genes (*MaF3h*, *MaDfr* and *MaAns*) that encode enzymes necessary for the biosynthesis of red anthocyanin pigment [47].

Consistent with these results, genetic variation in *MaMyb2* significantly co-segregates with floral anthocyanin production in F₂ hybrids generated from a cross between red-flowered *flemingii* and yellow-flowered *aridus* (ordinal logistic regression, likelihood ratio $\chi^2 = 127.5$; d.f. = 2; $p < 0.0001$, $R^2 = 0.39$; figure 2*a*). In addition, we found significantly elevated expression of *MaMyb2* and its putative targets in both *flemingii* and *puniceus* relative to the yellow-flowered taxa (figure 2*b*). We used virus-induced gene silencing (VIGS) to show that this change in gene expression at *MaMyb2* was necessary for the production of red flowers in *flemingii*, just as it was for *puniceus* [47]. By post-transcriptionally knocking down *MaMyb2* expression in *flemingii*, we revealed greatly reduced anthocyanin production in floral tissue (figure 2*c*), which resulted in significantly lower expression of *MaMyb2* and its putative target genes relative to negative controls (figure 2*d*). Finally, to determine whether differences in *MaMyb2* floral expression could be attributed to *cis*- or *trans*-acting mutations, we examined variation in allele-specific expression among F₁ heterozygotes. A significant allelic imbalance would indicate *cis*-regulation, whereas similar expression of both alleles would demonstrate a mutation acting in *trans* [51]. In flowers of F₁ hybrids between *flemingii* and either yellow-flowered *australis* or *aridus*, transcripts containing the *flemingii* allele were significantly over-represented relative to transcripts containing the *australis* or *aridus* allele (Fisher's exact test comparing allele frequencies in cDNA relative to gDNA; $p < 10^{-7}$ in five F₁S; electronic supplementary material, table S3).

These results demonstrate that red flowers in *puniceus* and *flemingii* are both controlled by *cis*-regulatory mutations in *MaMyb2*. However, determining whether these are due to the same or different mutations will require extensive functional testing of candidate SNPs using transgenic approaches, something that is not yet feasible in *M. aurantiacus*. Regardless, the history of *MaMyb2* divergence across the species complex appears noteworthy, in that red flowers either arose independently in each lineage because of separate gain-of-function mutations in *MaMyb2* or there was a single mutation that was subsequently shared between lineages.

(c) Divergence of *MaMyb2* between *puniceus* and *australis* is not consistent with their recent shared history

Although previous evidence revealed that the derived, red *MaMyb2* allele became fixed in *puniceus* due to positive selection by pollinators [47], the conditions surrounding its origin are not clear. One possible explanation is that a novel mutation arose in the ancestor of *puniceus* in an environment

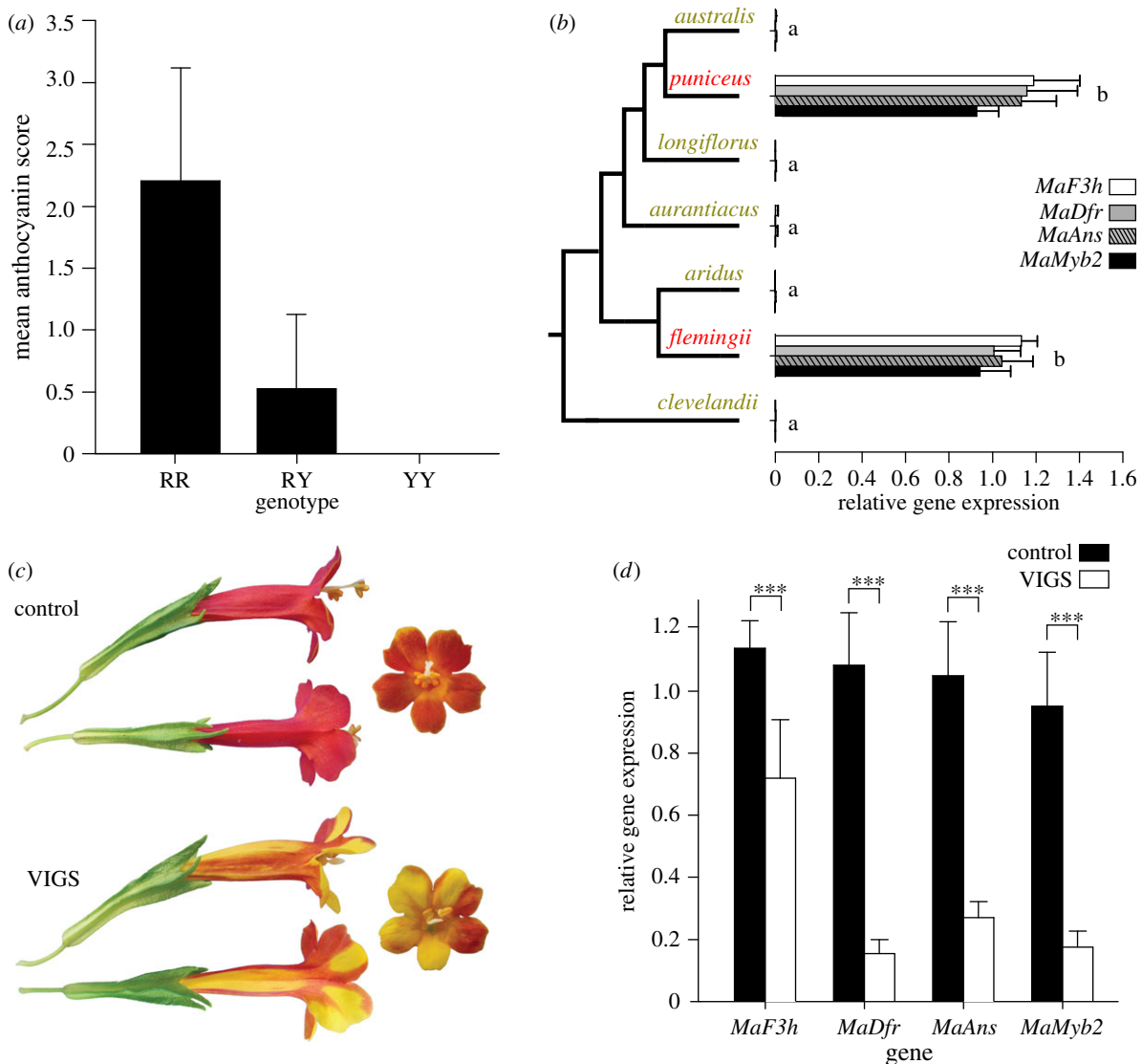


Figure 2. *MaMyb2* controls flower colour in *flemingii*. (a) Genotype at *MaMyb2* explains variation in floral anthocyanin production in F_2 hybrids between *flemingii* and *aridus*. Mean phenotypic scores (± 1 s.d.) are plotted for each genotype at a SNP marker in *MaMyb2* diagnostic for either the *flemingii* or the *aridus* grand-parental allele (R or Y, respectively). (b) Floral expression of *MaMyb2* and its putative target genes is significantly elevated in red flowers of *puniceus* and *flemingii* relative to the yellow-flowered subspecies. Error bars represent one standard error. Similar letters connect genes that are not statistically different from each other. (c) Representative photos in side, top, and front view of *flemingii* flowers in either the control group (top) or *MaMyb2*-silenced group (bottom) from VIGS experiments. (d) Compared to negative controls (black bars), *MaMyb2* VIGS silencing (white bars) leads to significantly fewer floral transcripts of *MaMyb2* and its putative targets. Error bars represent one standard error; asterisks represent $p < 0.001$ for all genes. (Online version in colour.)

that strongly favoured it, leading to its rapid fixation. This scenario predicts low levels of haplotype diversity in gene regions that are tightly linked to the causal mutation. Alternatively, the red *MaMyb2* allele may have been present in an ancestral *australis* population as standing variation prior to it having been favoured by selection. In this scenario, the causal element is likely to be found on many different haplotypes.

To test these expectations, we investigated patterns of *MaMyb2* haplotype variation between *puniceus* and *australis*. Despite gene flow between the subspecies, variants in *MaMyb2* are known to be tightly associated with flower colour differences [47], allowing us to use sequence data to make inferences about the origin of derived red flowers in *puniceus*. We observed very low haplotype diversity in *puniceus*, with a single *MaMyb2* haplotype found in nearly all samples (29/32 = 91% of sequenced alleles; figure 3). By contrast, we recovered 15 different haplotypes from 40 sampled *australis* alleles (frequency range 2.5–35%). This reduction in *MaMyb2* diversity cannot be attributed to a

recent demographic bottleneck in the ancestor of *puniceus*, as both subspecies have similar levels of genome-wide nucleotide diversity across populations (mean $\pi_{puniceus} = 0.00148 \pm \text{s.d. } 2.03 \times 10^{-4}$; mean $\pi_{australis} = 0.00141 \pm \text{s.d. } 2.59 \times 10^{-4}$). In addition, the presence of a single, high frequency *MaMyb2* haplotype in *puniceus* is not consistent with the red allele having existed as standing variation in an ancestral population of *australis*. Instead, these patterns support the rapid spread of a novel *MaMyb2* allele in *puniceus* due to a recent selective sweep that caused this segment of the gene to rise to high frequency.

The recent shared history between *puniceus* and *australis* (figure 1) predicts that *MaMyb2* sequences from *puniceus* should closely resemble sequences that are present in modern-day *australis*. However, we observed no haplotype sharing and 10 differentially fixed sites between *puniceus* and *australis* (figure 3). The presence of any fixed differences is striking given that none were found in a genome-wide comparison that surveyed more than 740 kb and 14 000

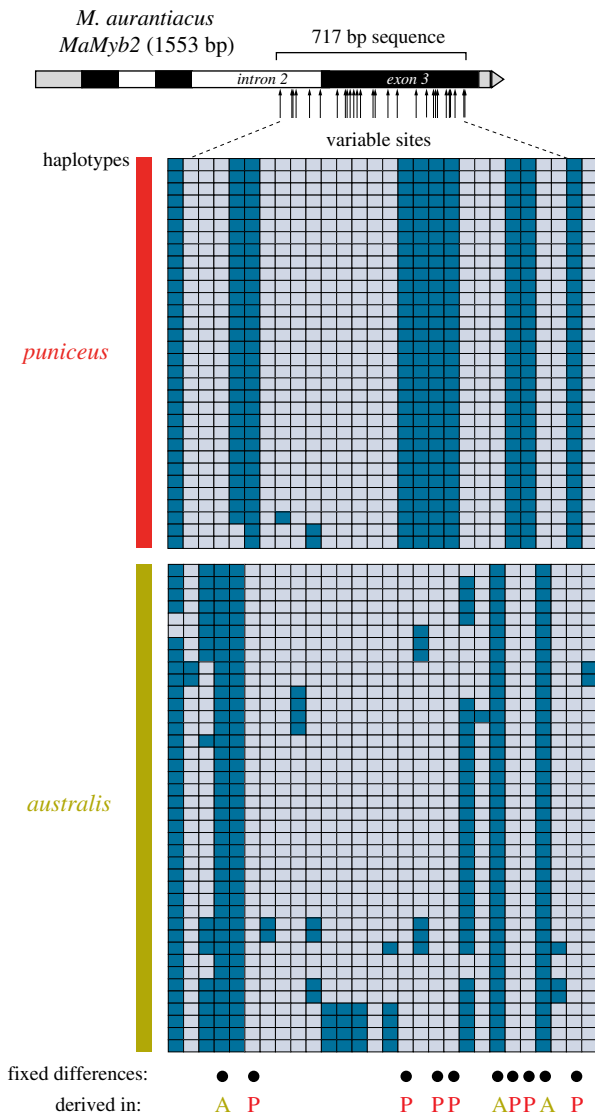


Figure 3. Divergence of *MaMyb2* between *puniceus* and *australis* is not consistent with their recent shared history. The diagram at the top shows the structure of the *MaMyb2* gene, with the location of the sequenced region indicated, along with arrows depicting the relative position of the 28 variable sites between *puniceus* and *australis*. Grey boxes represent 5' and 3' untranslated regions, and black and white boxes indicate exons and introns, respectively. Each row in the main diagram shows a phased haplotype including only the segregating sites from 16 *puniceus* and 20 *australis* individuals. Each segregating site is depicted as a grey or blue box that represents ancestral or derived sites, respectively, as determined by comparison with sequence from the *M. clevelandii* outgroup. Black circles indicate the position of the 10 differentially fixed sites, with the site labelled as A or P to represent whether the derived nucleotide is found in *australis* or *puniceus*, respectively. (Online version in colour.)

SNPs across 18 individuals from each subspecies [42]. As a consequence, the level of sequence divergence at *MaMyb2* is an order of magnitude greater than the genome-wide average (mean *p*-distance, *MaMyb2*: $0.0160 \pm \text{s.d. } 0.002$; genome-wide: $0.00150 \pm \text{s.d. } 0.00037$). Moreover, when the 10 differentially fixed sites were polarized as ancestral or derived relative to the *M. clevelandii* outgroup, the derived SNP was found in *australis* three times and in *puniceus* seven times (figure 3). Based on the recent shared ancestry of *puniceus* and *australis*, it is unexpected to find nucleotides that are derived and fixed in *australis* but absent from *puniceus*. Thus, although these data provide compelling support for

recent, strong selection on the red-flowered allele in *puniceus*, we conclude that this allele did not evolve *de novo* from a sequence that was present in its yellow-flowered ancestor. Rather, it appears that the common *MaMyb2* haplotype found in *puniceus* originated at some other point in the evolutionary history of the species complex. The subsequent sharing of this haplotype with *puniceus* could have occurred either through introgressive hybridization with a third subspecies, which transferred the haplotype to the ancestor of *puniceus*, or through lineage sorting, which resulted in the fixation of an ancestral red allele in *puniceus*.

(d) *MaMyb2* was transferred between divergent subspecies via introgressive hybridization

To identify the potential source of the divergent *MaMyb2* sequences recovered from *puniceus*, we sequenced the same region of *MaMyb2* in the remaining six subspecies (electronic supplementary material, table S1) and constructed a network of the phased haplotypes based on the number of nucleotide differences between them. Of the 152 sequenced *MaMyb2* alleles, we recovered 53 unique haplotypes separated by a maximum of 32 mutational steps (4.5% divergence; figure 4a). In general, haplotypes sampled from each of the four clades tended to group together and were separated from neighbouring haplotypes by fewer connections than those recovered from different clades. Moreover, only a single haplotype was shared between subspecies (electronic supplementary material, figure S3). By contrast, the haplotypes recovered from *puniceus* represented the only exception, as they differed from the haplotypes recovered from Clade D by at least 10 changes (figure 4a). These data provide further evidence that the red allele in *puniceus* is not derived from a locally evolved yellow-flowered allele that pre-existed in Clade D. Instead, the *puniceus* haplotypes grouped with the haplotypes recovered from Clade B, which contained the red-flowered *flemingii* and the yellow-flowered *aridus*.

The random sorting of a red *MaMyb2* allele that arose much earlier (i.e. in the ancestor of Clades B, C and D; node I, figure 1b) could explain a shared genetic basis for red flowers in both *flemingii* and *puniceus*. However, instead of finding *MaMyb2* haplotypes that were shared among clades, we observed patterns consistent with the complete sorting of *MaMyb2* variation across clades and subsequent lineage-specific sequence evolution (figure 4a). Indeed, with the exception of only the *puniceus* haplotypes, the major groups in the *MaMyb2* gene network were completely associated with the four primary clades in our subspecies tree (figure 4a). Alternatively, an ancestral red *MaMyb2* allele may have sorted differentially among lineages due to variation in selection pressures across the range of *M. aurantiacus*. This would have required the long-term maintenance of red and yellow *MaMyb2* alleles by balancing selection, followed by at least five independent losses of red flowers since the common ancestor of Clades B and D (Node I). Moreover, if the red allele that eventually fixed in *puniceus* was maintained as a polymorphism over this timescale, we would expect it to be present on many haplotypes due to the effects of mutation and recombination. However, as discussed above, the presence of a single, high frequency *MaMyb2* haplotype in *puniceus* contradicts our expectations that the red allele was maintained as a balanced polymorphism prior to sweeping to fixation in *puniceus*. Therefore, our data do not support the differential

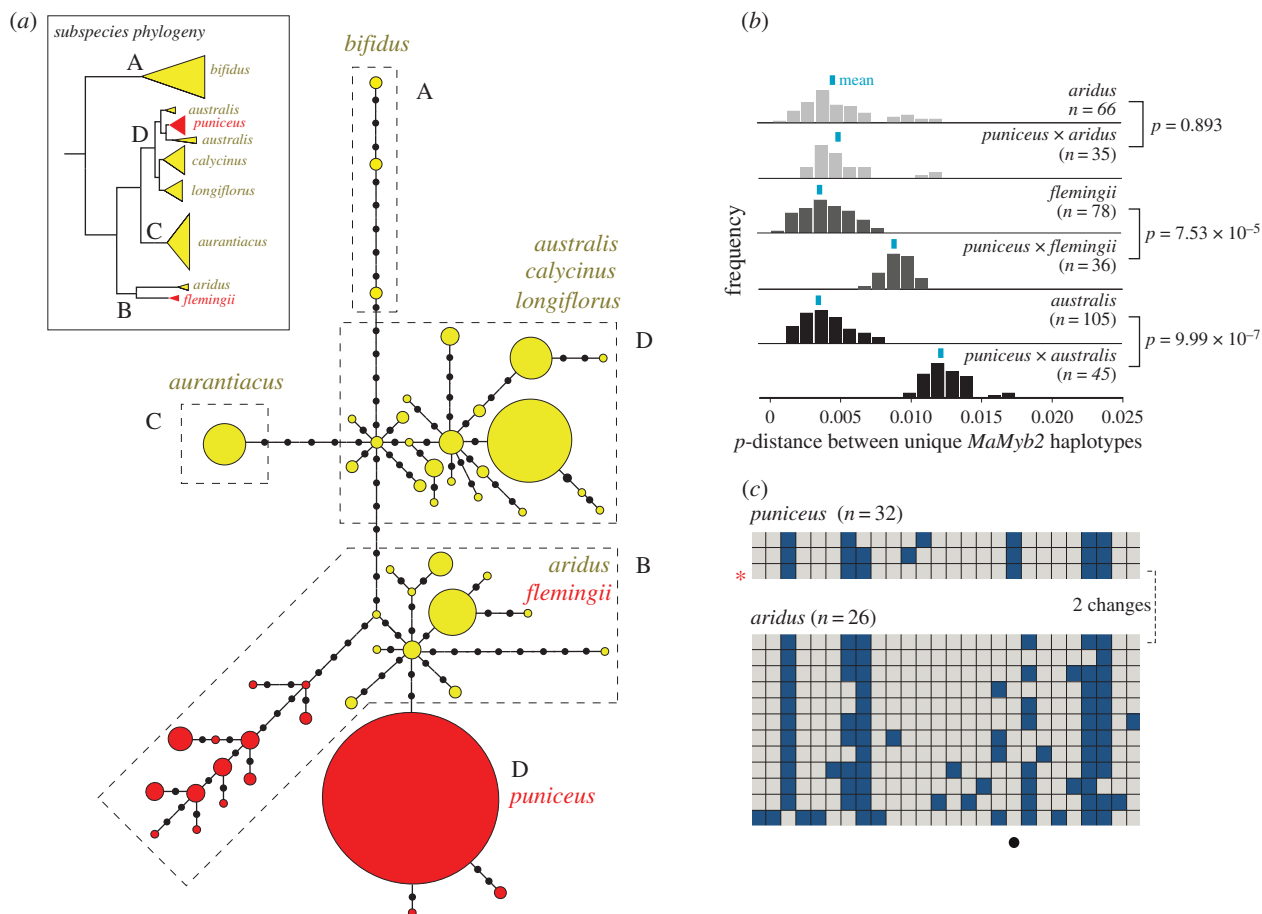


Figure 4. Introgressive hybridization has led to the transfer of *MaMyb2* into *puniceus*. (a) Haplotype network based on the number of differences among the 53 unique *MaMyb2* haplotypes recovered from 76 individuals across all eight subspecies. Each haplotype is represented by a circle, the size of which is proportional to its observed frequency. Colours correspond to flower colour, coded as anthocyanins present (red) or absent (yellow), as determined in electronic supplementary material, figure S2. Black circles show the number of mutational steps separating haplotypes. Dashed polygons enclose haplotypes recovered from each of the four major clades, as depicted in the inset phylogeny cartoon redrawn from figure 1. (b) Pairwise sequence divergence at *MaMyb2* among unique haplotypes. Frequency distributions of *p*-distance (the proportion of sites that differ between haplotypes) are plotted for comparisons within and between subspecies. Sample size reflects the number of pairwise estimates made for that comparison, and differences in the means (blue bar) between comparisons were tested using a permutation test with 10 000 randomizations. (c) Haplotype structure between *puniceus* and *aridus*. Only unique haplotypes within each subspecies are shown, with the colour coding of ancestral and derived sites the same as in figure 3. The common haplotype in *puniceus* is indicated by a red star. Sample sizes are indicated and represent the number of gene copies sequenced in each subspecies. The *aridus* haplotype that is most similar to the common *puniceus* haplotype is presented first and differs by only two changes, one of which is fixed and private to *puniceus* (black circle). (Online version in colour.)

sorting of an ancestral polymorphism as the source of the red *MaMyb2* allele in *puniceus*.

Rather, the discordant position of *puniceus* haplotypes in the *MaMyb2* network indicates that an ancestral individual from Clade B transferred the haplotype to *puniceus* via introgressive hybridization. Because the introgression event occurred in the past, subsequent sequence evolution and/or extinction prevent us from identifying the precise donor sequence. However, due to the recent radiation of the complex, we predicted that haplotypes in the modern-day descendants of the donor would remain similar to those found in *puniceus*. Interestingly, although *flemingii* also has red flowers, mean sequence divergence at *MaMyb2* between *puniceus* and *flemingii* is greater than the levels observed within *flemingii* ($p < 7.53 \times 10^{-5}$; permutation test; figure 4b, electronic supplementary material, figure S3). By contrast, mean pairwise divergence between *puniceus* and *aridus* ($0.46\% \pm \text{s.d. } 0.23$) is not significantly different from the diversity found among *aridus* haplotypes ($0.43\% \pm \text{s.d. } 0.27$; $p = 0.893$; permutation test). Moreover, despite the complex structure of the 10 fixed differences between *puniceus* and *aurantiacus* (figure 3), or the

six fixed differences between *puniceus* and *flemingii* (electronic supplementary material, figure S3), only a single substitution distinguishes the *puniceus* haplotypes from those recovered in *aridus* (figure 4c). These results indicate that *flemingii* is unlikely to be the modern-day descendant of the donor. Rather, the similarity of the *puniceus* and *aridus* haplotypes, and their discordance with *flemingii*, reveals that an ancestral *aridus*-like individual transferred the *MaMyb2* haplotype to *puniceus*.

Even though it is surprising that the *MaMyb2* sequences from *puniceus* are more similar to those found in yellow-flowered *aridus* than they are to red-flowered *flemingii* (figure 4b), our data are consistent with the potential for hybridization among these taxa based on their current geographical ranges (figure 1a). In particular, *flemingii* occurs only on the Channel Islands off the coast of California and does not co-occur with *puniceus* or *aurantiacus*. By contrast, *aridus* is distributed in a narrow region adjacent to the eastern edge of the *aurantiacus* range [52], suggesting that hybridization between them may have been possible in the recent past. Although historical ranges may have differed, which could lead to other possibilities, the most likely scenario to explain

our results is that an *aridus*-like individual transferred the red *MaMyb2* allele directly to *puniceus*, giving the allele an immediate selective advantage. An alternative possibility is that the introgressed region conferred yellow flowers at the time it was transferred to *puniceus*, but a novel *cis*-regulatory mutation arose in *MaMyb2* on the introgressed haplotype to give *puniceus* its red flowers. While we cannot rule this scenario out, the *cis*-regulatory mutation would have had to occur on that rare haplotype almost immediately after introgression to account for the remarkable similarities of haplotypes in *puniceus* and *aridus*. Thus, based on current evidence, it seems likely that a red *MaMyb2* allele arose once in the common ancestor of *flemingii* and *aridus* but was lost from *aridus* after it was transferred to *puniceus*. Future genomic analyses of this region, coupled with functional assays of regulatory elements, will allow us to conduct a more detailed test of this hypothesis.

3. Conclusion

In this study, our analysis of genome-wide variation suggested that red flowers evolved twice independently during the radiation of the *M. aurantiacus* species complex. However, in each case, a *cis*-regulatory mutation in the gene *MaMyb2* activated the expression of the same three enzymes, leading to the production of anthocyanin pigments in floral tissue. While these transitions in flower colour might reflect two independent gain-of-function mutations that each arose during the relatively short history of this group, our data do not indicate that the red-flowered allele in *puniceus* evolved *de novo* from a sequence already present in its yellow-flowered ancestor. Moreover, the occurrence of a single, high-frequency *MaMyb2* haplotype in *puniceus* that is remarkably similar to those recovered from *aridus* is not consistent with selection acting on a retained ancestral polymorphism. Therefore, although most population genetic models of adaptation contend that natural selection operates either on new mutations or on standing genetic variation that is already present in the population [6–8], our data support a scenario where a red *MaMyb2* allele was introgressed into *puniceus* following hybridization with a now extinct red-flowered individual from Clade B. The fact that the allele is not found in *australis* despite ongoing gene flow is consistent with a prominent role for natural selection by hummingbird and hawkmoth pollinators that display strong, opposing preferences for flowers of *puniceus* and *australis*, respectively [42,45,47].

It has been argued for nearly a century that adaptive genetic variation is frequently transferred across taxonomic boundaries due to introgressive hybridization [12,13,15–19,53]. Recent examples from a diversity of systems reveal that introgression can result in the spread of adaptations between distinct taxa [21,23,24,54,55]. However, in *Heliconius* butterflies, introgressed wing pattern loci contribute to both predator avoidance and pre-mating isolation [25,26], providing one of the only examples where introgressive hybridization has facilitated local adaptation while simultaneously promoting divergence [12,27,56]. Our results suggest that introgression of the red *MaMyb2* allele into the ancestor of *puniceus* was a primary driver of pollinator-mediated divergence that has led to the initial stages of reproductive isolation. This is further supported by the fact that the genomes of *puniceus* and *australis* are largely undifferentiated, implying that a few key loci such as *MaMyb2* have been critical for divergence [42,47]. Moreover,

as a consequence of the recent radiation in the *M. aurantiacus* species complex, taxa have retained the potential to exchange genes with each other, which has allowed for the spread of an allele that facilitated adaptive divergence.

4. Material and methods

(a) Genomic methods and data processing

We sequenced restriction-site associated DNA (RAD) tags from a single individual from 60 populations among the eight subspecies of *M. aurantiacus* and the outgroup, *M. clevelandii* (electronic supplementary material, table S1). DNA isolations and RAD library preparation followed the methods in [57] and have been described in [42]. Loci were created with the *denovo_map.pl* script in *Stacks* v. 1.06, with three identical raw reads required to create a stack, up to three mismatches allowed between loci for an individual, and up to eight mismatches allowed when joining loci among individuals. From this, single nucleotide polymorphisms (SNPs) were identified and genotypes called for each individual using the *populations* program in *Stacks*, requiring that loci were present at a minimum depth of $8\times$ in more than 90% of samples.

(b) Phylogenetic and population genomic analyses

Four different methods of phylogenetic reconstruction were used to infer the evolutionary relationships among the genotyped individuals: maximum-likelihood, Bayesian, neighbour joining and coalescent. Analyses were conducted using either the complete dataset of 41 528 SNPs or were further filtered to include 915 bi-allelic SNPs found on different tags that had minor allele frequencies greater than 0.1 and were present in 58 of the 60 populations. In addition to the tree-based methods, we ran a Bayesian model-based clustering algorithm, implemented in the program *Structure*, as well as a principal components analysis, to examine patterns of genotypic clustering among individuals. Finally, to examine the levels of genomic differentiation among the four primary clades (see Results and discussion), we estimated average pairwise F_{ST} and the total number (and proportion) of segregating sites that were fixed between each pair of clades. Details of each analysis can be found in the electronic supplementary material.

(c) Ancestral state reconstruction

We performed an ancestral state reconstruction to infer the number and direction of evolutionary transitions in flower colour during the radiation of *M. aurantiacus*. Character states (presence or absence of red anthocyanin pigment) were determined from extractions of total floral anthocyanidins using 200 mg of fresh corolla tissue from each of the in-group taxa and *M. clevelandii*, following methods described in [58,59]. Pigment extracts were adsorbed onto a cellulose thin layer chromatography plate and resolved using Forestal solvent [59]. We used a one-parameter maximum-likelihood model, implemented in Mesquite v. 3.01, to infer the relative probabilities of each character state at each node of the maximum-likelihood tree.

(d) Genetics of red flowers in *flemingii*

To determine whether genetic variation in *MaMyb2* was associated with floral anthocyanin production in *flemingii*, we tested for an association between *MaMyb2* genotype and floral anthocyanin production in 146 F_2 hybrids generated from a cross between red-flowered *flemingii* and yellow-flowered *aridus*. Using quantitative real-time PCR (QPCR), we then assayed for differences among subspecies in floral expression of *MaMyb2*, as well as three anthocyanin pathway genes (*MaF3h*, *MaDfr* and *MaAns*) known to have higher expression in *puniceus* relative

to *australis* [47,58]. To examine whether changes in *MaMyb2* gene expression were necessary for elevated floral anthocyanin production, we post-transcriptionally silenced *MaMyb2* in flowers of *flemingii* using a VIGS system that we described previously for *puniceus* [47]. Relative gene expression of *MaMyb2*, *MaF3h*, *MaDfr* and *MaAns* between VIGS and control flowers was quantified using QPCR. To determine whether elevated *MaMyb2* expression in *flemingii* flowers could be attributed to *cis*- or *trans*-acting factors, we followed methods described in [47] to compare allelic differences in *MaMyb2* expression in F₁ hybrids between red-flowered *flemingii* and either yellow-flowered *australis* or *aridus*. Details of all analyses can be found in the electronic supplementary material.

(e) *MaMyb2* sequencing

We used Sanger sequencing of purified PCR products to obtain a 717-bp region of *MaMyb2* from *M. clevelandii* and 76 individuals across all eight *M. aurantiacus* subspecies (electronic supplementary material, table S1). Previous analyses have demonstrated that SNP markers in this segment of the gene are tightly associated with flower colour differences between *puniceus* and *australis* [47]. Sequences were checked manually for quality and heterozygotes called from double peaks in the chromatograms. Because our analyses primarily examined population genetic questions related to sequence divergence among *puniceus*, *australis*, *flemingii* and *aridus*, we most heavily sampled from populations within these taxa (electronic supplementary material, table S1). PCR primers used were: 5'-TTGGGTACTGACCTAGTTGG-3' and 5'-CTTTG GAGGAATAGTCCAAGT-3'.

(f) Population genetic analyses

MaMyb2 sequences were aligned manually and haplotypes inferred using the program PHASE, as implemented in DNASP v. 5.10 [60]. Insertion–deletion polymorphisms were included in the analyses and coded as present or absent. We polarized derived and ancestral nucleotide changes relative to the *M. clevelandii* sequence. Mean pairwise levels of sequence divergence were estimated between *puniceus* and *australis* using Mega v. 6. These were compared to genome-wide estimates of pairwise

divergence between subspecies by re-analysing a previously published RADseq dataset [42]. This analysis consisted of Illumina sequenced RAD-tags from six individuals from each of three populations within each subspecies and resulted in 14 398 SNPs segregating in 7989 different 95-bp regions across the genome. Pairwise sequence divergence across the 758 955 sequenced sites was calculated in Mega v. 6, and mean estimates of nucleotide diversity (π) across populations within each subspecies were calculated in *Stacks v. 1.06*.

We constructed a *MaMyb2* haplotype network from all recovered haplotypes among subspecies based on an infinite site model and uncorrected distances using the *Pegas* package in R [61]. All connections were reconstructed with a probability greater than 0.97.

To determine the most likely modern descendant of the donor for the *MaMyb2* haplotypes recovered in *puniceus*, we estimated levels of pairwise sequence divergence among unique haplotypes within three potential donor subspecies: *australis*, *flemingii* and *aridus*. We then obtained estimates of pairwise sequence divergence between unique *puniceus* haplotypes and potential donor haplotypes. Mean estimates of divergence within and between subspecies were compared to null distributions based on 10 000 permutations of the data, as implemented in a custom script in R.

Data accessibility. All data from the article have been made publicly available on Dryad (<http://dx.doi.org/10.5061/dryad.33mp5>), GenBank (KT355497–KT355573) and on the Sequence Read Archive: (SRX1121822).

Authors' contributions. M.A.S. designed the experiments. S.S. and M.A.S. analysed the data and wrote the manuscript.

Competing interests. The authors declare no competing interests.

Funding. This project was supported by the University of Oregon and National Science Foundation awards DEB-1258199 and DEB-1311686 to M.A.S.

Acknowledgements. We thank Josh Bahr and Stephanie Le for assistance with data collection; Chris Smith for support with RAD sequencing; William Bradshaw, William Cresko, Christina Holzapfel, Keith Karoly, Thomas Nelson, Anne Royer, Chris Smith, Stacey Smith, James Sobel, Suzanne Renner and two anonymous reviewers for comments on previous versions of this manuscript.

References

- Chan YF *et al.* 2010 Adaptive evolution of pelvic reduction in sticklebacks by recurrent deletion of a *Pitx1* enhancer. *Science* **327**, 302–305. (doi:10.1126/science.1182213)
- Hopkins R, Rausher MD. 2011 Identification of two genes causing reinforcement in the Texas wildflower *Phlox drummondii*. *Nature* **469**, 411–414. (doi:10.1038/nature09641)
- Rebeiz M, Pool JE, Kassner VA, Aquadro CF, Carroll SB. 2009 Stepwise modification of a modular enhancer underlies adaptation in a *Drosophila* population. *Science* **326**, 1663–1667. (doi:10.1126/science.1178357)
- Stern DL, Orgogozo V. 2008 The loci of evolution: how predictable is genetic evolution? *Evolution* **62**, 2155–2177. (doi:10.1111/j.1558-5646.2008.00450.x)
- Prasad KVSK *et al.* 2012 A gain-of-function polymorphism controlling complex traits and fitness in nature. *Science* **337**, 1081–1084. (doi:10.1126/science.1221636)
- Hermisson J, Pennings PS. 2005 Soft sweeps: molecular population genetics of adaptation from standing genetic variation. *Genetics* **169**, 2335–2352. (doi:10.1534/genetics.104.036947)
- Hartl DL, Clark AG. 2007 *Principles of population genetics*, 4th edn. Sunderland, MA: Sinauer.
- Barrett RDH, Schluter D. 2008 Adaptation from standing genetic variation. *Trends Ecol. Evol.* **23**, 38–44. (doi:10.1016/j.tree.2007.09.008)
- Mayr E. 1963 *Animal species and evolution*. Cambridge, MA: Harvard University Press.
- Wagner WH. 1969 The role and taxonomic treatment of hybrids. *Bioscience* **19**, 785–795. (doi:10.2307/1294787)
- Dowling TE, Secor CL. 1997 The role of hybridization and introgression in the diversification of animals. *Annu. Rev. Ecol. Syst.* **28**, 593–619. (doi:10.1146/annurev.ecolsys.28.1.593)
- Abbott R *et al.* 2013 Hybridization and speciation. *J. Evol. Biol.* **26**, 229–246. (doi:10.1111/j.1420-9101.2012.02599.x)
- Rieseberg LH, Wendel J. 1993 Introgression and its consequences in plants. In *Hybrid zones and the evolutionary process* (ed. RG Harrison), pp. 70–109. Oxford, UK: Oxford University Press.
- Schemske DW. 2000 Understanding the origin of species. *Evolution* **54**, 1069–1073. (doi:10.1111/j.0014-3820.2000.tb00111.x)
- Anderson E. 1949 *Introgressive hybridization*. New York, NY: John Wiley and Sons.
- Anderson E, Stebbins GL Jr. 1954 Hybridization as an evolutionary stimulus. *Evolution* **8**, 378–388. (doi:10.2307/2405784)
- Arnold ML. 2004 Transfer and origin of adaptations through natural hybridization: were Anderson and Stebbins right? *Plant Cell* **16**, 562–570. (doi:10.1105/tpc.160370)
- Lewontin RC, Birch LC. 1966 Hybridization as a source of variation for adaptation to new environments. *Evolution* **20**, 315–336. (doi:10.2307/2406633)
- Heiser CB. 1973 Introgression reexamined. *Bot. Rev.* **39**, 347–366. (doi:10.1007/BF02859160)

20. Pialek J, Barton NH. 1997 The spread of an advantageous allele across a barrier: the effects of random drift and selection against heterozygotes. *Genetics* **145**, 493–504.
21. Hedrick PW. 2013 Adaptive introgression in animals: examples and comparison to new mutation and standing variation as sources of adaptive variation. *Mol. Ecol.* **22**, 4606–4618. (doi:10.1111/mec.12415)
22. Whitney KD, Randell RA, Rieseberg LH. 2010 Adaptive introgression of abiotic tolerance traits in the sunflower *Helianthus annuus*. *New Phytol.* **187**, 230–239. (doi:10.1111/j.1469-8137.2010.03234.x)
23. Kim M, Cui ML, Cubas P, Gillies A, Lee K, Chapman MA, Abbott RJ, Coen E. 2008 Regulatory genes control a key morphological and ecological trait transferred between species. *Science* **322**, 1116–1119. (doi:10.1126/science.1164371)
24. Kim SC, Rieseberg LH. 1999 Genetic architecture of species differences in annual sunflowers: implications for adaptive trait introgression. *Genetics* **153**, 965–977.
25. Heliconius Genome Consortium. 2012 Butterfly genome reveals promiscuous exchange of mimicry adaptations among species. *Nature* **487**, 94–98.
26. Pardo-Diaz C, Salazar C, Baxter SW, Merot C, Figueiredo-Ready W, Joron M, McMillan WO, Jiggins CD. 2012 Adaptive introgression across species boundaries in *Heliconius* butterflies. *PLoS Genet.* **8**, e1002752. (doi:10.1371/journal.pgen.1002752)
27. Lamichaney S *et al.* 2015 Evolution of Darwin's finches and their beaks revealed by genome sequencing. *Nature* **518**, 371–375. (doi:10.1038/nature14181)
28. Schluter D. 2001 Ecology and the origin of species. *Trends Ecol. Evol.* **16**, 372–380. (doi:10.1016/S0169-5347(01)02198-X)
29. Nosil P, Harmon LJ, Seehausen O. 2009 Ecological explanations for (incomplete) speciation. *Trends Ecol. Evol.* **24**, 145–156. (doi:10.1016/j.tree.2008.10.011)
30. Rundle HD, Nosil P. 2005 Ecological speciation. *Ecol. Lett.* **8**, 336–352. (doi:10.1111/j.1461-0248.2004.00715.x)
31. Feder JL, Xie XF, Rull J, Velez S, Forbes A, Leung B, Dambroski H, Filchak KE, Aluja M. 2005 Mayr, Dobzhansky, and Bush and the complexities of sympatric speciation in *Rhagoletis*. *Proc. Natl Acad. Sci. USA* **102**, 6573–6580. (doi:10.1073/pnas.0502099102)
32. Coyne JA, Orr HA. 2004 *Speciation*. Sunderland, MA: Sinauer.
33. Nosil P. 2012 *Ecological speciation*. Oxford, UK: Oxford University Press.
34. Nosil P. 2008 Speciation with gene flow could be common. *Mol. Ecol.* **17**, 2103–2106. (doi:10.1111/j.1365-294X.2008.03715.x)
35. Via S. 2009 Natural selection in action during speciation. *Proc. Natl Acad. Sci. USA* **106**, 9939–9946. (doi:10.1073/pnas.0901397106)
36. Beardsley PM, Schoenig SE, Whittall JB, Olmstead RG. 2004 Patterns of evolution in Western North American *Mimulus* (Phymaceae). *Am. J. Bot.* **91**, 474–489. (doi:10.3732/ajb.91.3.474)
37. Pritchard JK, Stephens M, Donnelly P. 2000 Inference of population structure using multilocus genotype data. *Genetics* **155**, 945–959.
38. McMinn HE. 1951 Studies in the genus *Diplacus*, Scrophulariaceae. *Madrono* **11**, 33–128.
39. Beeks RM. 1962 Variation and hybridization in southern California populations of *Diplacus* (Scrophulariaceae). *El Aliso* **5**, 83–122.
40. Thompson DM. 1993 *Mimulus*. In *The Jepson manual; higher plants of California* (ed. JC Hickman), pp. 1037–1047. Los Angeles, CA: University of California Press.
41. Tulig M. 2000 Morphological variation in *Mimulus* section *Diplacus* (Scrophulariaceae). MS thesis, California State Polytechnic University, Pomona.
42. Sobel JM, Streisfeld MA. 2015 Strong premating reproductive isolation drives incipient speciation in *Mimulus aurantiacus*. *Evolution* **69**, 447–461. (doi:10.1111/evo.12589)
43. Grant V. 1981 *Plant speciation*, 2 edn. New York, NY: Columbia University Press.
44. Grant V. 1993 Origin of floral isolation between ornithophilous and sphingophilous plant species. *Proc. Natl Acad. Sci. USA* **90**, 7729–7733. (doi:10.1073/pnas.90.16.7729)
45. Streisfeld MA, Kohn JR. 2007 Environment and pollinator-mediated selection on parapatric floral races of *Mimulus aurantiacus*. *J. Evol. Biol.* **20**, 122–132. (doi:10.1111/j.1420-9101.2006.01216.x)
46. Streisfeld MA, Kohn JR. 2005 Contrasting patterns of floral and molecular variation across a cline in *Mimulus aurantiacus*. *Evolution* **59**, 2548–2559. (doi:10.1111/j.0014-3820.2005.tb00968.x)
47. Streisfeld MA, Young WN, Sobel JM. 2013 Divergent selection drives genetic differentiation in an R2R3-MYB transcription factor that contributes to incipient speciation in *Mimulus aurantiacus*. *PLoS Genet.* **9**, e1003385. (doi:10.1371/journal.pgen.1003385)
48. Martin SH *et al.* 2013 Genome-wide evidence for speciation with gene flow in *Heliconius* butterflies. *Genome Res.* **23**, 1817–1828. (doi:10.1101/gr.159426.113)
49. Brawand D *et al.* 2014 The genomic substrate for adaptive radiation in African cichlid fish. *Nature* **513**, 375–381. (doi:10.1038/nature13726)
50. Munz PA, Keck DD. 1973 *A California flora and supplement*. Berkeley, CA: University of California Press.
51. Wittkopp PJ, Haerum BK, Clark AG. 2004 Evolutionary changes in *cis* and *trans* gene regulation. *Nature* **430**, 85–88. (doi:10.1038/nature02698)
52. Thompson DM. 2005 Systematics of *Mimulus* subgenus *Schizoplacus* (Scrophulariaceae). *Syst. Bot. Monogr.* **75**, 1–213.
53. Mallet J. 2005 Hybridization as an invasion of the genome. *Trends Ecol. Evol.* **20**, 229–237. (doi:10.1016/j.tree.2005.02.010)
54. Green RE *et al.* 2010 A draft sequence of the Neandertal genome. *Science* **328**, 710–722. (doi:10.1126/science.1188021)
55. Huerta-Sanchez E *et al.* 2014 Altitude adaptation in Tibetans caused by introgression of Denisovan-like DNA. *Nature* **512**, 194–197. (doi:10.1038/nature13408)
56. Schumer M, Rosenthal GG, Andolfatto P. 2014 How common is homoploid hybrid speciation? *Evolution* **68**, 1553–1560. (doi:10.1111/evo.12399)
57. Etter PD, Bassham S, Hohenlohe PA, Johnson EA, Cresko WA. 2011 SNP discovery and genotyping for evolutionary genetics using RAD sequencing. *Methods Mol. Biol.* **772**, 157–178. (doi:10.1007/978-1-61779-228-1_9)
58. Streisfeld MA, Rauscher MD. 2009 Altered *trans*-regulatory control of gene expression in multiple anthocyanin genes contributes to adaptive flower color evolution in *Mimulus aurantiacus*. *Mol. Biol. Evol.* **26**, 433–444. (doi:10.1093/molbev/msn268)
59. Harborne JB. 1984 *Phytochemical methods*, 2nd edn. New York, NY: Chapman and Hall.
60. Librado P, Rozas J. 2009 DnaSP v5: a software for comprehensive analysis of DNA polymorphism data. *Bioinformatics* **25**, 1451–1452. (doi:10.1093/bioinformatics/btp187)
61. Paradis E. 2010 pegas: an R package for population genetics with an integrated-modular approach. *Bioinformatics* **26**, 419–420. (doi:10.1093/bioinformatics/btp696)